Lipid Oxidation during Thermogenesis in High-Altitude Deer Mice (*Peromyscus maniculatus*)

Sulayman A. Lyons[1], Kevin B. Tate [1], Kenneth C. Welch Jr.[2] and Grant B. McClelland[1]

[1]Department of Biology, McMaster University, Hamilton, ON, L8S 4K1, Canada
[2]Department of Biological Sciences, University of Toronto Scarborough, M1C 1A4, ON, Canada

Corresponding author: Sulayman Lyons, McMaster University, Department of Biology, 1280 Main Street West, Hamilton, ON L8S 4K1, Canada. Email: lyonssa@mcmaster.ca

Running title: LIPID OXIDATION IN THERMOREGULATING HIGH-ALTITUDE DEER MICE

Key words: Cold-induced $\dot{V}O_2max$, summit metabolism, substrate utilization, fat oxidation

Abstract

When at their maximum thermogenic capacity (cold-induced $\dot{V}O_2max$), small endotherms reach levels of aerobic metabolism as high, or even higher, than running $\dot{V}O_2max$. How these high rates of thermogenesis are supported by substrate oxidation is currently unclear. The appropriate utilization of metabolic fuels that could sustain thermogenesis over extended periods may be important for survival in cold environments, like high altitude. Previous studies show that high capacities for lipid use in high-altitude deer mice may have evolved in concert with greater thermogenic capacities. The purpose of this study was to determine how lipid utilization at both moderate and maximal thermogenic intensities may differ in high- and low-altitude deer mice, and strictly low-altitude white-footed mice. We also examined the phenotypic plasticity of lipid use after acclimation to cold hypoxia (CH), conditions simulating high altitude. We found that lipids were the primary fuel supporting both moderate and maximal rates of thermogenesis in both species of mice. Lipid oxidation increased 3-fold in mice from 30°C to 0°C, consistent with increases in oxidation of [^{13}C]-palmitic acid. CH acclimation led to an increase in [^{13}C]-palmitic acid oxidation at 30°C but did not affect total lipid oxidation. Lipid oxidation rates at cold-induced $\dot{V}O_2max$ were two- to four-fold those at 0°C and increased further after CH acclimation, especially in high-altitude deer mice. These are the highest mass-specific lipid oxidation rates observed in any land mammal. Uncovering the mechanisms that allow for these high rates of oxidation will aid our understanding of the regulation of lipid metabolism.

Introduction

Homeothermic endothermy is a distinctive feature of mammals that is crucial for their survival in cold environments. However, thermal tolerance and thermogenic capacity are performance traits that not only vary with body size but also with individual and population differences in thermal history (23, 31, 54). For instance, small mammals have greater thermoregulatory costs compared to larger species due to a higher surface area for heat loss relative to volume used for heat production. This can be especially challenging for species that are active during colder parts of the year, necessitating high rates of thermogenesis to remain active when temperatures are low (15, 28). Past research has uncovered many details on how these species can maintain high rates of O_2 delivery to thermogenic tissues (21). However, it remains unclear how metabolic substrates are utilized to support high rates of thermogenesis in mammals or if fuel use patterns change seasonally.

Thermogenesis is an aerobic process that allows endotherms to maintain stable body temperatures by balancing heat lost to the external environment with endogenous heat production. The onset of thermogenesis occurs when the ambient temperature falls below an endotherm's thermoneutral zone (54) and can occur in two major ways, shivering and non-shivering thermogenesis (NST). Shivering thermogenesis increases metabolic demand via muscular contractions that provide heat but no beneficial locomotory work, while NST produces heat through the futile cycling of protons across the mitochondrial membrane via uncoupling protein 1 in brown adipose tissue (BAT) (12). While shivering is fueled by both carbohydrates and lipids, depending on shivering intensity (25), NST is primarily fueled by lipids (8, 32). Furthermore, prolonged cold exposure increases shivering capacity (45) and elevate BAT metabolic activity (5, 62).

Endogenous lipid stores are large in mammals (~80% available energy reserves) and it has been speculated that lipids may be used to sustain heat production (63). Data from rats show that during modest cold exposure (5^{o}C), lipid oxidation supports over 50% of the metabolic demand of shivering thermogenesis (61). However, we are not aware of any study examining fuel use for thermogenesis in smaller mammals, such as mice. It is well-characterized in mammals that maximal rates of lipid oxidation during locomotion occur at moderate intensities of aerobic exercise (10, 53, 65), and these rates do not vary even if fat availability is artificially elevated (26). Although during exercise higher mass-specific rates of lipid oxidation are observed in mice compared to larger species, they too demonstrate an upper limit to lipid use at submaximal exercise intensities (33, 53, 60). Interestingly, during cold-induced $\dot{V}$O2max (also referred to as summit metabolism) small endotherms often reach levels of aerobic metabolism higher than $\dot{V}O_2$max elicited by exercise (15, 27, 37). This suggests that metabolism supporting even moderate rates of thermogenesis may be higher than those during aerobic exercise, when lipid oxidation plateaus or even declines (64). Whether small mammals can sustain sufficient rates of lipid oxidation to support even these moderate rates of thermogenesis is unclear.

High-altitude environments can be cooler year-round than lower elevations of the same latitude. Yet, populations of small mammals native to high altitude, such as deer mice, remain active in the cold, maintaining higher daily energetic costs compared to low altitude conspecifics, even during summer months (28). There is also evidence of directional selection for greater cold-induced $\dot{V}O_2$max in deer mice at high altitude (29), and thermogenic capacity in hypoxia is higher in high-altitude deer mice compared to lowland conspecifics (18, 19, 57). This superior aerobic capacity at high altitude is the product of environmentally induced phenotypic plasticity overlaid upon fixed population differences (19, 34, 58). While the oxygen transport

pathway from the external environment to muscle tissues have been extensively examined in mammals living at high altitude (38), fuel use has received much less attention. However, work examining exercise metabolism in high altitude conditions suggests a greater reliance in carbohydrates to support submaximal locomotion, presumably as an oxygen-saving strategy. This has been demonstrated in two species in the genus *Phyllotis* native to the high Andes (53) and in deer mice native to the Rocky Mountains, born and raised at low altitude and acclimated to chronic hypoxia (33). However, how metabolic fuel use may have evolved at altitude to support the high rates of thermogenesis is currently not well understood.

It would be unlikely that a preferential utilization of carbohydrate oxidation occurs to support the high rates of thermogenesis at high altitude, given mammals have limited glycogen reserves (37), and the prolonged nature of thermoregulation would quickly deplete these stores. Indeed, after a 6-week acclimation to low altitude conditions, wild high-altitude native deer mice showed respiratory exchange ratios (RER= $\dot{V}CO_2/\dot{V}O_2$) at cold-induced $\dot{V}O_2max$ in hypoxia suggestive of a high reliance on lipids (18). These high proportions of lipid use may be largely influenced by NST activity in BAT. Moreover, the higher thermogenic capacities in high-altitude mice suggests a corresponding elevated rate of lipid oxidation. Phenotypic differences between low- and high-altitude deer mice in the gastrocnemius, a muscle used in thermogenesis (44), suggest higher capacities for fatty acid oxidation at high altitude, presumably to support high rates of shivering (18, 33).

Whether moderate and/or maximal rates of heat production are supported solely by lipids or a combination of metabolic fuels has not been explored in either low or high-altitude deer mice. Moreover, it is unclear if lipid oxidation rates follow the same population differences in

aerobic capacity, or if this fuel utilization for heat production is affected by acclimation to simulated high-altitude conditions.

To address these issues, we used deer mice (*Peromyscus maniculatus*) native to high altitude and compared them to a low-altitude population and to a closely related strictly low-altitude species, the white-footed mouse (*P. leucopus*). Mice were born and raised in common low-altitude conditions and acclimated as adults to cold hypoxia simulating high altitude. We tested the hypothesis that moderate and maximal rates of thermogenesis are predominately supported by lipid metabolism in deer mice and rates of lipid oxidation are higher in deer mice native to high altitude. High-altitude deer mice are also predicted to respond to chronic cold hypoxia with a greater increase in lipid oxidation during thermogenesis than low-altitude mice.

Materials and Methods

Animals and experimental design

Male and female deer mice and white-footed mice used in this study were first generation descendants of wild-caught *P.m. rufinus* trapped at the summit of Mount Evans CO (4,350m a.s.l.) and *P.m. nebracensis and P. leucopus* trapped at low altitude at Nine-mile Prairie, NE, USA (320m a.s.l.). Mice were born and raised at McMaster University (~90m a.s.l.) in common laboratory conditions of ~23^{o}C, light cycle of 12:12h light:dark, food and water ad libitum. All mice were at least 6 months of age before the start of experiments. This experimental design allows us to separate the effects of altitude ancestry and environment on physiological traits (18, 33, 34, 58). All procedures were approved by the McMaster University Animal Research Ethics Board in accordance with guidelines from the Canadian Council on Animal Care.

168 *Acclimation Conditions*

169 First generation high-altitude (HA) and low-altitude (LA) deer mice were randomly
170 divided into two acclimation groups and kept for 6 to 8 weeks in either, 1) warm normoxia
171 (WN), at 23°C and 760mmHg (21kPa O_2) - our common laboratory conditions, or 2) cold
172 hypoxia (CH), at 5°C and 480mmHg (12kPa O_2) using hypobaric chambers (35) housed in a
173 climate controlled room to simulate an altitude of 4300m a.s.l. Mice in the CH group were first
174 placed in a cold room for 24 hours at normobaria to adjust to the cold before being placed in the
175 hypobaric chambers. Mice in CH were returned to normobaria in cold for a brief period (<1h)
176 twice a week to clean cages and replenish food and water (57, 58).
177
178 *Respirometry*

179 Open-flow respirometry was used to determine rates of oxygen consumption ($\dot{V}O_2$) and
180 CO_2 production ($\dot{V}CO_2$). For each mouse, $\dot{V}O_2$ and $\dot{V}CO_2$ were measured at thermoneutral
181 temperatures (30°C) (16) and moderate cold temperatures (0°C) using a PTC-1 Portable
182 Controlled Temperature Cabinet (Sable Systems, Las Vegas, NV) in random order. Mice were
183 made post-absorptive by a 4-6 hour fast, weighed and placed in a respirometry chamber
184 (~500ml). Dry (Drierite, Hammond, OH) and CO_2 free (Soda Lime and Ascarite, Thomas
185 Scientific, NJ) air was flowed (pushed) into the respirometry chamber at 600ml min^{-1}, using a
186 mass-flow controller (Sable Systems). Excurrent air was subsampled at a rate of ~200ml min^{-1},
187 dried using pre-baked Drierite (67), and passed through O_2 and CO_2 analyzers (Sable Systems).
188 Fractional incurrent O_2 (F_{iO_2}) and CO_2 (F_{iCO_2}) were recorded at the beginning and end of the trial
189 by flowing air through an empty respirometry chamber. After mice adjusted to the chamber for
190 20 minutes, fractional excurrent concentrations of O_2 (F_{eO_2}) and CO_2 (F_{eCO_2}) were determined for

20 minutes and $\dot{V}O_2$ and $\dot{V}CO_2$ were calculated using equation 3b from Withers (68). Body temperatures were measured before and after all experimental trials using a rectal probe thermometer (RET-3-ISO, Physitemp). Resting $\dot{V}O_2$ was defined as the lowest, most stable reading during a 1.5 min interval during the last 20 minutes of the trial. Whole-animal rates of substrate oxidation were calculated using the indirect calorimetry equations from Frayn (22) assuming a minimal contribution of protein oxidation in the post absorptive state (11, 24). Protein oxidation has been shown to contribute only ~5% to energy production during exercise in post-absorptive mammals. Thus, we assumed no contribution of protein oxidation when calculating rates of fuel oxidation. Thermal conductance (C) was calculated based on equations from Scholander et al. (54).

Hypoxic cold-induced $\dot{V}O_2$max reported here are from Tate et al. (58) with an additional 5 HA and 5 LA mice in WN and 9 HA and 9 LA mice in CH. Cold-induced $\dot{V}O_2$max was determined by flowing heliox (21% O_2, 79% He or 12% O_2, 88% He), at 1000ml min^{-1} using mass flow meters and controllers (Sierra Instruments, Monterey, CA, USA; MFC-4, Sable Systems, NV, USA), through copper coils housed inside a temperature control cabinet and into a glass respirometry chamber (~500ml) cooled to ~-10^{o}C. Heliox induces greater heat loss at warmer temperatures and avoids the risk of cold injury to the animals (17, 51). Mice were exposed to these conditions for ~15 minutes and cold-induced $\dot{V}O_2$max was defined as the peak value of $\dot{V}O_2$ averaged over a 10-15 second period (50, 57).

All mice were given at least 48 hours to recover before another submaximal or cold-induced $\dot{V}O_2$max trial was performed.

^{13}C Stable Isotope Breath Analysis

Using indirect calorimetry can provide an estimate of whole-body lipid oxidation rate. While these rates are still very informative, they do not directly quantify the rate of oxidation of specific fuels or sources. We labelled endogenous fat stores with [^{13}C]-palmitate and quantified rates of [^{13}C]-palmitate oxidation by collecting exhaled $^{13}CO_2$ and measuring $\dot{V}CO_2$, as previously described for other species (40, 43). Using this approach, we could quantify how the rate of oxidation of labelled lipid stores specifically varied with ancestry, acclimation or acute thermal challenge. Briefly, labelled food was prepared by completely dissolving 0.5g of [1-^{13}C]-palmitic acid (Cambridge Isotope Laboratories, Inc) in 95% ethanol to coat 0.5kg of rodent chow (front and back). The chow was then baked at 60^{o}C overnight. A subset of mice was fasted up to a maximum of 24 hours with full access to water to heavily deplete endogenous lipid stores (41, 55). After the 24-hour fast, or once mouse weight was ~80% of their original body mass, animals were provided the ^{13}C-labelled chow for at least 10 days to replenish and ensure sufficient labeling of endogenous lipid stores. Mice were given labelled chow until all breath sampling trial data were collected.

Breath samples were collected from animals before and after [^{13}C]-palmitic acid enrichment of fat stores. Food was removed 4 hours prior to collection of breath $^{13}CO_2$ to prevent recently ingested ^{13}C from influencing our determination of endogenous lipid use (42). During respirometry trials at 30^{o}C and 0^{o}C, a 12ml subsample of excurrent air was collected from these mice using a gas-tight glass syringe and transferred to a 12ml glass exetainer (Labco). Breath samples were analyzed for δ^{13}C signatures by cavity ring-down spectroscopy using the Picarro G2201-I Isotopic Analyzer (Picarro, Inc., Santa Clara, CA, USA). Using the techniques and equations provided by Dick et al. (20) and McCue et al. (40), δ^{13}C signatures were used to calculate [^{13}C]-palmitic acid oxidation (43).

237

238 *Measurement of Plasma Fatty Acids*

239 Blood samples were obtained from the submandibular vein immediately following
240 indirect calorimetry trials at 30°C and 0°C. Blood was immediately centrifuged at 10,000 × g for
241 5 min to separate red cells from plasma. Plasma was quickly frozen in liquid nitrogen and stored
242 until further analysis. To quantify free fatty acids, 20µl of plasma were combined with 10µl of
243 internal standard (C17:0, 0.6mg ml^{-1}) in 1ml of 2,2-dimethoxypropane and vortexed. This was
244 followed by the addition of 40µl of HCl (12M) and the methylation of free fatty acids was left to
245 proceed for 1h. The reaction was stopped with the addition of 20µl of pyridine and vortexed.
246 Next, 750µl of iso-octane and 500µl of dH_2O was added to the samples, and then centrifuged at
247 10,000 × g for 5 min. The resultant upper phase was transferred to a new tube, and the process
248 was repeated for the bottom layer. The top phases were combined and completely dried under
249 N_2. The sample was re-suspended in 50µl of iso-octane and transferred to an autosampler tube.
250 Another 50µl of iso-octane was added to the original sample tube to re-suspend any remaining
251 contents and was also transferred to the autosampler tube and was completely dried under N_2.
252 The final sample was re-suspended in 50µl of iso-octane (36).

253 Samples were analyzed using an Agilent Technologies 6890N gas chromatograph with a
254 30m fused silica capillary column (DB-23, Agilent Technologies), flame ionization detector and
255 equipped with an automatic injection system (Agilent Technologies 7683B Series). Helium was
256 used as the carrier gas at a constant pressure and column velocity of 44cm s^{-1}, with 4µl of sample
257 injected into the column. The conditions used during analysis were the following: oven
258 temperature initially programmed for 4min at 160°C, ramped to 220°C at a rate of 2°C min^{-1} and
259 held at 220°C for 2 min, then ramped to 240°C at 10°C min^{-1}, and held at 240°C for 7 min. Post-

run was 130°C for 4 min. The detector temperature was 250°C. Identities of fatty acid methyl esters were compared to the retention times of a standard FAME mix (C8-C24, Sigma). We excluded analysis of fatty acids less than 16 carbons as we did not attempt to minimize volatilization (47).

Statistics

Linear mixed effects models were used to test for effects of population, acclimation, and experimental temperature. Analyses were performed using the lme4 package (3) in R v.4.0.0 (59). We assessed the potential interactions between fixed factors, including body mass as a covariate and the random effects of family, sex and age. If the variance explained by random effects did not approach significance ($p>0.05$), we removed them and reran the analysis. Except for body mass, all other dependant variables were reduced to 3-way analysis of variance (ANOVA)s, with mass as a covariate where appropriate. Additionally, within each experimental temperature (30°C and 0°C), and cold-induced $\dot{V}O_2max$ condition (normoxia and hypoxia), 2-way ANOVAs were performed assessing the interaction between population and acclimation. Pairwise, Holm Sidak post hoc tests were performed to assess significant interactions (30). All statistical analyses were performed on the absolute values of the traits that were not corrected for body mass, but some data are presented as relative to body mass by convention to the literature ($\dot{V}O_2$, $\dot{V}O_2max$, ventilatory volumes, [^{13}C]-palmitate oxidation, lipid oxidation and thermal conductance). All data are presented as mean ± sem. A statistical significance value was set at $P<0.05$.

Results

Body Mass

White-footed mice weighed 29% more than both HA and LA deer mice, regardless of acclimation environment ($p<0.05$) (Table 1). However, there was no significant difference in mass between HA and LA deer mice ($p>0.05$) (Table 1).

Respiration in thermoneutral and moderate cold temperatures

To determine if altitude ancestry or acclimation to CH influences metabolic rate during submaximal thermogenesis, we measured $\dot{V}O_2$ at thermoneutrality (30ºC) and during a moderate cold exposure (0ºC) in LA and HA deer mice and white-footed mice. We found that $\dot{V}O_2$ was 3-fold greater at 0°C compared to 30°C for all individuals, regardless of population and acclimation environment ($p<0.05$). HA and LA deer mice had greater $\dot{V}O_2$ than white-footed mice at both 30°C and 0°C ($p<0.05$), but there were no differences in $\dot{V}O_2$ between HA and LA deer mice ($p>0.05$). Furthermore, acclimation did not significantly influence $\dot{V}O_2$ ($p>0.05$) (*Fig. 1A*). We calculated RER during these submaximal rates of thermogenesis and found it was unaffected by ambient temperature ($p>0.05$). While all mice tested at 0°C had similar RERs regardless of population or acclimation ($p>0.05$), at 30°C white-footed mice acclimated to CH had higher RER than those housed in WN ($P<0.05$). The range of RERs observed in all trials were between 0.70 to 0.80 across all groups, suggesting that lipids were the primary source of fuel in thermoneutral conditions and with moderate cold exposure (*Fig. 1B*).

Whole animal lipid oxidation rates during submaximal thermogenesis

Since lipid oxidation is the primary fuel for both shivering and non-shivering thermogenesis in rodents (18, 61), we determined if altitude ancestry or acclimation environment influenced this trait in moderate cold conditions. Using indirect calorimetry, we calculated whole-animal lipid oxidation rates and observed an increase from 30°C to 0°C ($p<0.05$). Across all temperatures, LA deer mice had greater lipid oxidation rates compared to white-footed mice ($p<0.05$), but not compared to HA deer mice ($p>0.05$). At 30°C, both HA and LA deer mice had greater lipid oxidation rates compared to white-footed mice ($p<0.05$). Interestingly, CH acclimation did not affect whole-animal rates of lipid oxidation ($p>0.05$) (*Fig. 2A*).

Thermal conductance during submaximal thermogenesis

Thermal conductance was calculated to determine if changes in rates of heat loss occurred due to exposure to colder ambient temperatures with CH acclimation (*Table 1*). We found that thermal conductance was reduced as ambient temperature decreased from 30°C to 0°C ($F_{1,79} = 147.67$, $P<0.001$), while controlling for any influence of body mass ($F_{1,79} = 21.16$, $P<0.001$). Across all temperatures, white-footed mice had greater thermal conductance compared to HA and LA deer mice ($F_{2,79} = 16.43$, $P<0.001$), which led to greater changes in body temperature after moderate cold exposure ($p<0.05$). Acclimation to CH had no effect on thermal conductance ($F_{1,79} = 0.866$, $P=0.355$) (*Table 1*).

[^{13}C]- palmitic acid oxidation

We directly quantified the oxidation of an individual fatty acid by labelling the fat stores in a subset of LA and HA deer mice using [^{13}C]-palmitate and trapping exhaled $^{13}CO_2$ during submaximal thermogenic trials. We found, similar to whole-animal lipid oxidation, that [^{13}C]-

palmitate oxidation rates increased 3-fold as ambient temperatures declined from 30°C to 0°C ($p<0.05$). However, in contrast to whole-animal lipid oxidation rates, CH acclimation led to an increase in [^{13}C]-palmitate oxidization ($p<0.05$). Specifically, at 30°C [^{13}C]-palmitate oxidation increased in CH acclimated HA mice compared to their WN controls ($p<0.05$) (*Fig. 2B*).

Circulating plasma non-esterified fatty acids

To understand if substrate use was reflected in changes of circulating plasma non-esterified fatty acids (NEFAs), we determined levels of total and individual circulating NEFAs (*Fig. 2C and Fig. 3*). Overall, plasma concentrations of total circulating NEFAs did not change as ambient temperature decreased ($p>0.05$), nor were there any significant effects of population ($p>0.05$) or acclimation ($p>0.05$) (*Fig. 2C*).

Similar to total NEFA, plasma concentrations of palmitate (16:0) and stearate (18:0) showed no differences between populations, acclimation or with changes in ambient temperature ($p>0.05$; *Fig. 3A and Fig.3C*). In contrast, palmitoleate (16:1) was ~47% higher in LA deer mice than HA deer mice at 30°C ($p<0.05$). The concentration of palmitoleate was also significantly higher in CH acclimated mice at 0°C ($p<0.05$; *Fig. 3B*). Elaidate (18:1n9t) concentrations were found to be higher in HA deer mice, while oleate (18:1n9c) concentrations were higher in LA deer mice ($p<0.05$; *Fig. 3D; Fig. 3E*). Concentrations of oleate were also significantly greater in CH acclimated mice at 0°C but significantly greater in WN animals at 30°C ($p<0.05$) (*Fig. 3E*). Linoleate (18:2n6c) concentrations were relatively constant with no significant effect of acclimation or temperature ($p>0.05$); however, generally HA mice had higher levels of linoleate compared to LA mice ($p<0.05$; *Fig. 3F*).

354 *Whole animal lipid oxidation at cold-induced $\dot{V}O_2max$*

355 Thermogenic capacity was assessed by measuring cold-induced $\dot{V}O_2max$. We determined
356 $\dot{V}O_2$ and lipid oxidation rates at $\dot{V}O_2max$ in both normoxia and hypoxia. After accounting for
357 differences in body mass ($F_{1,135} = 16.93$, $P<0.001$), we found that $\dot{V}O_2max$ was higher in
358 normoxia compared to hypoxia ($F_{1,135} = 353.22$, $P<0.001$). After CH acclimation, $\dot{V}O_2max$
359 increased ($F_{1,135} = 201.44$, $P<0.001$), but there were no significant population differences ($F_{2,135} =$
360 2.80, P=0.064) (*Fig. 4A*).

361 RER at $\dot{V}O_2max$ was higher in normoxia compared to hypoxia ($F_{1,136} = 9.46$, $P<0.001$).
362 There was a significant population × acclimation × test condition interaction in RER ($F_{1,136}$
363 =3.80, P=0.025), where WN HA mice tested in normoxia had greater RERs than WN HA mice,
364 CH white-footed mice and WN white-footed mice when tested in hypoxia ($p<0.05$). In normoxia,
365 there was a significant population × acclimation interaction ($F_{2,40} = 4.10$, P=0.024), where CH
366 acclimation led to a decrease in RER in HA mice ($p<0.05$), while WN LA mice had lower RERs
367 than WN HA mice ($p<0.05$). In hypoxia, RER was not different among populations or with
368 acclimation environment (*Fig. 4B*).

369 Whole-animal lipid oxidation rates at $\dot{V}O_2max$ were higher in normoxia compared to
370 hypoxic conditions ($p<0.05$). In addition, mice acclimated to CH had greater lipid oxidation rates
371 compared to WN individuals ($p<0.05$). In normoxia, HA deer mice acclimated to CH displayed
372 higher lipid oxidation rates compared to WN white-footed mice ($p<0.05$). In hypoxia, HA deer
373 mice had higher lipid oxidation rates than LA mice, and CH acclimation led to an increase lipid
374 oxidation ($p<0.05$; *Fig. 4C*).

375

376

Discussion

The main objective of this study was to determine the substrate utilization necessary to support both moderate and maximal intensities of thermogenesis in LA and HA native *Peromyscus* mice and how this utilization is influenced by acclimation to CH, simulating high altitude. We found that both deer mice and white-footed mice significantly increase whole body lipid oxidation rates from thermoneutral (30^{o}C) to moderate cold (0^{o}C) to support heat production. At 0^{o}C, lipid oxidation accounted for the majority of total $\dot{V}O_2$ but did not differ among the three mouse populations. There was also no effect of CH acclimation on the proportional use of lipid oxidation at this moderate cold exposure. However, when the oxidation of a major circulating free fatty acid was measured directly through $^{13}CO_2$ production, we found CH acclimation led to a significant increase in palmitate oxidation at 30^{o}C when compared to WN acclimated controls. At cold-induced $\dot{V}O_2$max under hypoxia, we found whole-animal lipid oxidation rates were elevated two- to four-fold above moderate cold in WN and CH HA deer mice, respectively. This population also showed a significant effect of CH acclimation leading to higher whole-animal lipid oxidation at $\dot{V}O_2$max in normoxia. These results demonstrate that lipid oxidation is the major fuel supporting thermogenesis in deer mice, even at maximal cold-induced metabolic rates. Indeed, rates of lipid oxidation that support heat production at 0^{o}C are similar or greater than maximal rates observed during moderate exercise intensities (33). Furthermore, oxidation rates to support maximal thermogenesis were 2.5 to 5.2-fold greater than maximal rates of lipid oxidation during exercise (21; *Fig. 5*) and the highest mass-specific lipid oxidation rates reported for any mammal (1, 33, 49, 61).

400 *Submaximal and Maximal Thermogenic Metabolism*

401 Thermoregulation allows for endotherms to balance rates of heat production and heat loss
402 to maintain consistent body temperatures (54). To maintain stable body temperatures as ambient
403 temperatures decrease, there must be an increase of both $\dot{V}O_2$ and substrate availability to match
404 the increased metabolic demand of thermoregulation (38, 57). We observed as the need for heat
405 generation increased, there was an increase in metabolic rate, but RERs remained constant and
406 between 0.7 and 0.8 in all mice. Mice also showed a decline in thermal conductance that reduced
407 rates of heat loss as ambient temperature decreased from thermoneutral (30^{o}C) to moderate cold
408 (0^{o}C) temperatures (*Fig.1; Table 1*), consistent with previous studies on small mammals (13, 14,
409 16, 48, 69). Interestingly, when exposed to moderate cold, both HA and LA deer mice had the
410 same $\dot{V}O_2$ and RERs, suggesting a specific amount of energy and fuel required for submaximal
411 thermogenic demand, which was maintained even after acclimation to CH.

412 When cold-induced $\dot{V}O_2$max was stimulated, RER remained low suggesting fuel utilization
413 did not change between moderate and maximal thermogenic requirements, despite the large
414 change in metabolic rate (*Fig. 4A,B*). Previous research has shown an adaptive advantage for
415 high aerobic capacity in HA deer mice (29), and that wild HA mice maintain higher hypoxic
416 $\dot{V}O_2$max than their LA conspecifics when tested in their native environments (19). We did not
417 find a significant difference in thermogenic capacity between laboratory born and raised HA and
418 LA mice (*Fig. 4A*). These results are consistent with previous measurements of hypoxic $\dot{V}O_2$max
419 in WN and CH acclimated deer mice (57, 58). However, when deer mice were acclimated to
420 warm hypoxia, HA mice did show higher hypoxic $\dot{V}O_2$max than both LA deer mice (57), and
421 white-footed mice (58). Although the combined effects of cold hypoxia can have opposing
422 effects on thermogenesis in laboratory mice (5), we found CH acclimation significantly

423 increased $\dot{V}O_2max$ in all populations. Given the evidence that higher thermogenic capacities are
424 under directional selection in deer mice at high altitude (29), having the ability to elevate
425 thermogenic capacity in response to cold would be adaptive for surviving alpine environments.
426
427 *Whole animal lipid oxidation rates*
428 The substrates used by mammals to support thermogenesis, and the rate they are oxidized
429 to support heat production, has received little attention. Here we provide data on substrate use
430 during moderate cooling and at peak thermogenesis in *Peromyscus*. All mice fuelled submaximal
431 thermogenesis primarily with lipids, which contributed between 70 to 93% of total metabolism.
432 At thermoneutrality, lipids supported only 59% of total energy requirements in white-footed
433 mice after CH acclimation (*Fig. 1B*). Nonetheless, these mice used lipid oxidation to a
434 proportionally greater extent to power thermogenesis than previously observed in rats exposed to
435 5^{o}C (*Fig. 5;* 43).
436 During moderate rates of thermogenesis, lipid oxidation rates were equivalent to maximal
437 rates observed during aerobic locomotion in the same species (*Fig.* 5; 22). Data from a number
438 of low altitude native mammals (humans, mice rats, goats and dogs) show that substrate use
439 during exercise follows a predictable pattern, where rates of lipid oxidation plateau at moderate
440 intensities (52). At higher exercise intensities, lipid use does not increase, even when fatty acid
441 availability is artificially increased (26). However, we show that during thermogenesis in deer
442 mice, lipid oxidation continues to increase and support higher metabolic rates to levels that are 5-
443 fold higher than those observed during exercise in this species (*Fig. 5*). These high rates of lipid
444 oxidation support both the activation of BAT metabolism and high rates of muscle shivering.
445 The degree that these tissues rely on either endogenous or circulatory sources of lipid fuel is

446 currently unclear. It is important to note that we determined lipid oxidation by indirect
447 calorimetry, which can become unreliable when animals leave steady state conditions at higher
448 metabolic rates (49). However, given the linear relationship between $\dot{V}O_2$ and total ventilation
449 across a range of thermogenic intensities (48) and ventilatory equivalents that never reach
450 anaerobic threshold (46, 70), our data suggests that thermoregulating mice in this study were in
451 steady state metabolism, even at cold-induced $\dot{V}O_2$max (*Fig S1, Table S1 and Table S2;*
452 Supplemental Material for this article can be found online at
453 https://doi.org/10.6084/m9.figshare.13564784).

454 The oxidation of [^{13}C]-palmitate was also directly quantified during moderate cold
455 exposures. From thermoneutral to moderate cold, we observed a three-fold increase of [^{13}C]-
456 palmitate oxidation (*Fig. 2B*), directly reflecting the increase in whole-animal lipid oxidation
457 (*Fig. 2A*). However, while total lipid oxidation was unaffected by acclimation in HA mice, [^{13}C]-
458 palmitate oxidation was higher in CH acclimated HA mice. Interestingly, plasma concentrations
459 of palmitate did not track changes in its oxidation but remained stable with acute changes in
460 temperature and with CH acclimation (*Fig. 3A*). This mismatch between whole-body palmitate
461 oxidation and circulating palmitate concentrations with thermogenic demand may shed some
462 light on how fatty acids are utilized to match demand for heat production. While difficulty in
463 interpreting experimentally induced changes in blood metabolites has been highlighted by others
464 (39), we suggest two potential explanations for our data. The first explanation suggests that rates
465 of palmitate disappearance into active tissues are tightly matched with rates of appearance into
466 plasma. The second explanation suggests CH leads to greater use of palmitate from endogenous
467 lipid stores within thermo-effector tissues, such as muscle and/or BAT. Measuring flux of

circulating fatty acids, along with the oxidation of both circulatory and intracellular sources of lipid will provide a deeper understanding of how lipid depots are used during thermogenesis.

Total plasma NEFA levels also remained constant, a reflection of changes in those individual fatty acids with high percent contributions to total NEFA (e.g., palmitate and stearate) (*Fig. 2C; Fig. 3*). However, HA mice showed higher plasma concentrations of elaidate and linoleate, but lower concentrations of palmitoleate and oleate, compared to LA deer mice (*Fig 3*). Acclimation to CH led to a selective increase in plasma levels of palmitoleate and oleate at 0^{o}C and a decrease in oleate at 30^{o}C. These findings suggest a population, acclimation, and temperature-specific mobilization of specific NEFA in deer mice.

At peak rates of thermogenesis, lipids were the predominant fuel used by all mice, regardless of altitude ancestry. Lipids constituted 67 to 100% to total oxygen use, regardless of acclimation environment (*Fig. 4B*). In hypoxia, highlanders showed higher lipid oxidation rates than lowland deer mice at $\dot{V}O_2$max, which further increased with CH acclimation (*Fig. 4C*). The capacity for high rates of lipid oxidation is likely an important feature of the HA phenotype, and along with an elevated $\dot{V}O_2$max (29), increases the probability of winter survival in HA deer mice. Similar to differences in $\dot{V}O_2$max (19), lipid oxidation in hypoxia was higher in HA deer mice due to a combined effect of phenotypic plasticity, overlaid upon genetic differences in maximal rates of fuel use. When the constraint of hypoxia was removed and thermogenic capacity was determined in normoxia, lipid oxidation at $\dot{V}O_2$max increased with CH in highlanders, to the highest mass-specific rates recorded for any mammal (*Fig. 4C*).

Mice used proportionally more lipids in hypoxia than in normoxia, with this fuel accounting for almost 100% of $\dot{V}O_2$ in some instances. These observations may appear paradoxical, given the higher ATP yield per mole of O_2 afforded by carbohydrate oxidation (9,

63) and their increased use with exercise observed in highland native mice (33, 53). However, the efficiency advantage of carbohydrates as a fuel is likely outweighed by the need of critical tissues for this limited resource (35). Instead, mobilization and utilization of lipids is increased in response to a prolonged need for metabolic heat production, even in face of low O_2 availability. Lipid reserves are in abundance in mammals (36) and could sustain prolonged thermogenesis at an ecologically relevant alpine ambient temperature of 0^{o}C (Western Regional Climate Centre), for up to 71 hours, assuming ~4g of stored lipids (20% of a 20g mouse). Our findings also suggest that even at maximal rates of heat production, onboard lipids would last up to 16 hours until fully depleted. These liberal estimates assume all lipids are accessible to the thermo-effector tissues. Nevertheless, mice are capable of oxidizing lipids at very high rates by delivering fatty acids to working mitochondria. How this process occurs is a fruitful area of future research.

The Lipid Oxidation Pathway

Elevated rates of lipid oxidation to support moderate and maximal rates of heat production require sufficient capacities for mobilization, transport, and oxidation to supply free fatty acids to working mitochondria. During exercise, maximal lipid oxidation is thought to be limited by fatty acid uptake across the sarcolemma of working muscle (64, 66) and mitochondrial membranes (4, 56). Both of these potential limitations may be bypassed during thermogenesis. Unlike exercise, where skeletal muscle accounts for ~80% of O_2 and substrate use (2), thermogenesis in small mammals involves both shivering by skeletal muscle and non-shivering thermogenesis, principally in BAT. Perhaps thermogenic tissues increase reliance on intracellular stores of lipids for fuelling thermogenesis. For example, BAT increases intracellular lipolysis with cold stress in both humans and rats (7, 8, 32). Alternatively, cold stress may

514 stimulate increased blood flow and increased capacity for fatty acid uptake for BAT and
515 shivering muscle (6). Acclimation to CH would further amplify these differences by increasing
516 BAT activity and increasing capacity for lipid transport and oxidation in BAT and muscle. Thus,
517 differences in fuel use between exercise and thermogenesis may involve the relative
518 contributions of these energy consuming tissues involved (21, 42). Indeed, further research is
519 needed to understand the mechanisms involved and determine how these components of the lipid
520 oxidation pathway are regulated during thermogenesis.
521
522
523 **Perspectives and Significance**
524 We report that lipid oxidation is the primary fuel supporting both moderate and maximal
525 rates of thermogenesis in both deer mice and white-footed mice. Rates of lipid oxidation also
526 reflect the higher thermogenic capacity in hypoxia of HA deer mice, suggesting capacity for high
527 lipid use has also evolved in this environment. In addition, we show that rates of lipid oxidation
528 during thermogenesis are much higher than during exercise and report the highest mass-specific
529 rates, observed in any land-dwelling mammal, to our knowledge. These results highlight a need
530 to understand how lipid oxidation is regulated during high rates of metabolic heat production.
531 For example, it is unknown how the limitation to maximal lipid oxidation observed during
532 exercise is circumvented when animals are thermoregulating. We suggest the increased reliance
533 on BAT activity is an important driver for the high reliance on lipid use during thermogenesis;
534 however, NST occurring in BAT accounts for ~50-60% of cold-induced $\dot{V}O_2$max in deer mice
535 (62) suggesting lipids used for shivering is more than twice that is observed during exercise (33).
536 Rates of lipid use by shivering muscles are likely much higher than those observed during

exercise. How these higher rates of oxidation are achieved are currently unclear. Animals in chronically cold environments, such as the high alpine, would also require a consistent supply of dietary nutrients to maintain the observed elevated daily metabolic rates (28). However, we know little about food sources available to HA deer mice or how they may differ from those at lower elevations. These next steps will provide a deeper understanding of how thermoregulation can raise the ceiling for fat oxidation, and ultimately provide more insight as to how these deer mice can survive the challenging environment of high-altitude.

Acknowledgements

The authors would like to thank G. Scott and C. Ivy for technical assistance and use of plethysmography equipment. We would also like to thank M. McCue for technical advice on stable isotope analysis and M. Dick for technical assistance with stable isotope analysis. Current address for K. Tate is the Department of Biology, Texas Lutheran University, Seguin, TX 78155, USA.

Author Contributions

S.A.L. and G.B.M. designed the study. S.A.L. performed experiments and analyzed data. K.B.T. collected hypoxic $\dot{V}O_2$max data. K.C.W. provided equipment and assisted with stable isotope analysis. S.A.L. and G.B.M. wrote the manuscript and all the authors edited the manuscript.

Funding

This work was funded by a Natural Sciences and Engineering Research Council of Canada (NSERC) Discovery Grant and a NSERC Discovery Accelerator Supplement (G.B.M.). S.A.L was supported by a NSERC Canada Graduate Scholarship.

References

1. **Achten J**, **Venables MC**, **Jeukendrup AE**. Fat oxidation rates are higher during running compared with cycling over a wide range of intensities. *Metabolism* 52: 747–752, 2003. doi: 10.1016/S0026-0495(03)00068-4.
2. **Armstrong RB, Essen-Gustavsson B, Hoppeler H, Jones JH, Kayar SR, Laughlin MH, Lindholm A, Longworth KE, Taylor CR, Weibel ER.** O_2 delivery at VO_2max and oxidative capacity in muscles of standardbred horses. *J Appl Physiol* 73(6): 2274-2282, 1992.
3. **Bates D**, **Mächler M**, **Bolker BM**, **Walker SC**. Fitting linear mixed-effects models using lme4. *J Stat Softw* 67, 2015. doi: 10.18637/jss.v067.i01.
4. **Båvenholm PN**, **Pigon J**, **Saha AK**, **Ruderman NB**, **Efendic S**. Malonyl-CoA in Human Muscle. *Ethics* 49, 2000.
5. **Beaudry JL**, **McClelland GB**. Thermogenesis in CD-1 mice after combined chronic hypoxia and cold acclimation. *Comp Biochem Physiol - B Biochem Mol Biol* 157: 301–309, 2010. doi: 10.1016/j.cbpb.2010.07.004.
6. **Blondin DP**, **Frisch F**, **Phoenix S**, **Guérin B**, **Turcotte ÉE**, **Haman F**, **Richard D**, **Carpentier AC**. Inhibition of Intracellular Triglyceride Lipolysis Suppresses Cold-Induced Brown Adipose Tissue Metabolism and Increases Shivering in Humans. *Cell Metab* 25: 438–447, 2017. doi: 10.1016/j.cmet.2016.12.005.
7. **Blondin DP**, **Labbé SM**, **Noll C**, **Kunach M**, **Phoenix S**, **Guérin B**, **Turcotte ÉE**, **Haman F**, **Richard D**, **Carpentier AC**. Selective impairment of glucose but not fatty acid or oxidative metabolism in brown adipose tissue of subjects with type 2 diabetes. *Diabetes* 64: 2388–2397, 2015. doi: 10.2337/db14-1651.

8. **Blondin DP**, **Labbé SM**, **Phoenix S**, **Guérin B**, **Turcotte ÉE**, **Richard D**, **Carpentier AC**, **Haman F**. Contributions of white and brown adipose tissues and skeletal muscles to acute cold-induced metabolic responses in healthy men. *J Physiol* 593: 701–714, 2015. doi: 10.1113/jphysiol.2014.283598.

9. **Brand MD**. The stoichiometry of proton pumping and synthesis in mitochondria. *Biochem (Lond)* 16: 20–24, 1994.

10. **Brooks GA, Mercier J.** Balance of carbohydrate and lipid utilization during exercise: the "crossover" concept. *J Appl Physiol* 76(6): 2253-2261, 1994.

11. **Bulow J**. *Lipid mobilization and utilization. In Principles of Exercise Biochemistry*. J.R. Poort. Basel: Karger, 1988.

12. **Cannon B**, **Nedergaard J**. Brown Adipose Tissue: Function and Physiological Significance. *Physiol Rev* 84: 277–359, 2004. doi: 10.1152/physrev.00015.2003.

13. **Casey TM, Withers PC, Casey KK.** Metabolic and respiratory responses of arctic mammals to ambient temprature during the summer. Comparative Biochemistry and Physiology--Part A: *Physiology* 64(3): 331-341, 1979.

14. **Chappell MA**. Effects of ambient temperature and altitude on ventilation and gas exchange in deer mice (Peromyscus maniculatus). *J Comp Physiol B* 155: 751–758, 1985. doi: 10.1007/BF00694590.

15. **Chappell MA**, **Hammond KA**. Maximal aerobic performance of deer mice in combined cold and exercise challenges. *J Comp Physiol B Biochem Syst Environ Physiol* 174: 41–48, 2004. doi: 10.1007/s00360-003-0387-z.

16. **Chappell MA**, **Holsclaw DS**. Effects of wind on thermoregulation and energy balance in deer mice (Peromyscus maniculatus). *J Comp Physiol B* 154: 619–625, 1984. doi:

614 10.1007/BF00684416.

615 17. **Chappell MA**, **Rezende EL**, **Hammond KA**. Age and aerobic performance in deer mice.
616 *J Exp Biol* 206: 1221–1231, 2003. doi: 10.1242/jeb.00255.

617 18. **Cheviron ZA**, **Bachman GC**, **Connaty AD**, **McClelland GB**, **Storz JF**. Regulatory
618 changes contribute to the adaptive enhancement of thermogenic capacity in high-altitude
619 deer mice. *Proc Natl Acad Sci* 109: 8635–8640, 2012. doi: 10.1073/pnas.1120523109.

620 19. **Cheviron ZA**, **Connaty AD**, **Mcclelland GB**, **Storz JF**. Functional genomics of
621 adaptation to hypoxic cold-stress in high-altitude deer mice: Transcriptomic plasticity and
622 thermogenic performance. *Evolution (N Y)* 68: 48–62, 2014. doi: 10.1111/evo.12257.

623 20. **Dick MF**, **Alcantara-Tangonan A**, **Oghli YS**, **Welch KC**. Metabolic partitioning of
624 sucrose and seasonal changes in fat turnover rate in ruby-throated hummingbirds
625 (Archilochus colubris). *J Exp Biol* 223, 2020. doi: 10.1242/jeb.212696.

626 21. **Foster DO**, **Frydman ML**. Tissue distribution of cold-induced thermogenesis in
627 conscious warm- or cold-acclimated rats reevaluated from changes in tissue blood flow:
628 The dominant role of brown adipose tissue in the replacement of shivering by
629 nonshivering thermogenesis. *Can J Physiol Pharmacol* 57: 257–270, 1979. doi:
630 10.1139/y79-039.

631 22. **Frayn KN**. Calculation of substrate oxidation rates in vivo from gaseous exchange. *J Appl*
632 *Physiol* 55(2):628-634, 1983.

633 23. **Fristoe TS**, **Burger JR**, **Balk MA**, **Khaliq I**, **Hof C**, **Brown JH**. Metabolic heat
634 production and thermal conductance are mass-independent adaptations to thermal
635 environment in birds and mammals. *Proc Natl Acad Sci U S A* 112: 15934–15939, 2015.
636 doi: 10.1073/pnas.1521662112.

637 24. **Gessaman JA**, **Nagy K.** Energy metabolism: errors in gas-exchange conversion factors.
638 *Physiol Zool* 61, 1988.
639 25. **Haman F**, **Legault SR**, **Weber JM**. Fuel selection during intense shivering in humans:
640 EMG pattern reflects carbohydrate oxidation. *J Physiol* 556: 305–313, 2004. doi:
641 10.1113/jphysiol.2003.055152.
642 26. **Hargreaves M**, **Kiens B**, **Richter EA**. Effect of increased plasma free fatty acid
643 concentration on muscle metabolism in exercising men. *J Appl Physiol* 70: 194–201,
644 1991. doi: 10.1152/jappl.1991.70.1.194.
645 27. **Hayes AJP**, **Chappell MA**,**Hayes JP**, **Chappell MA**. Individual Consistency of Maximal
646 Oxygen Consumption in Deer Mice *Funct Ecol* 4: 495–503, 1990.
647 28. **Hayes JP**. Altitudinal and seasonal effects on aerobic metabolism of deer mice. *J Comp*
648 *Physiol B* 159: 453–459, 1989. doi: 10.1007/BF00692417.
649 29. **Hayes JP**, **O'Connor CS**. Natural Selection on Thermogenic Capacity of High-Altitude
650 Deer Mice. *Evolution (N Y)* 53: 1280, 1999. doi: 10.2307/2640830.
651 30. **Hothorn T**, **Bretz F**, **Westfall P**. Simultaneous inference in general parametric models.
652 *Biom J* 50: 346–363, 2008.
653 31. **Khaliq I**, **Fritz SA**, **Prinzinger R**, **Pfenninger M**, **Böhning-Gaese K**, **Hof C**. Global
654 variation in thermal physiology of birds and mammals: Evidence for phylogenetic niche
655 conservatism only in the tropics. *J Biogeogr* 42: 2187–2196, 2015. doi:
656 10.1111/jbi.12573.
657 32. **Labbé SM**, **Caron A**, **Bakan I**, **Laplante M**, **Carpentier AC**, **Lecomte R**, **Richard D**.
658 In vivo measurement of energy substrate contribution to cold-induced brown adipose
659 tissue thermogenesis. *FASEB J* 29: 2046–2058, 2015. doi: 10.1096/fj.14-266247.

33. **Lau DS**, **Connaty AD**, **Mahalingam S**, **Wall N**, **Cheviron ZA**, **Storz JF**, **Scott GR**, **McClelland GB**. Acclimation to hypoxia increases carbohydrate use during exercise in high-altitude deer mice. *Am J Physiol - Regul Integr Comp Physiol* 312: R400–R411, 2017. doi: 10.1152/ajpregu.00365.2016.

34. **Lui MA**, **Mahalingam S**, **Patel P**, **Connaty AD**, **Ivy CM**, **Cheviron ZA**, **Storz JF**, **McClelland GB**, **Scott GR**. High-altitude ancestry and hypoxia acclimation have distinct effects on exercise capacity and muscle phenotype in deer mice. *Am J Physiol - Regul Integr Comp Physiol* 308: R779–R791, 2015. doi: 10.1152/ajpregu.00362.2014.

35. **McClelland GB**, **Hochachka PW**, **Weber J-M**. Carbohydrate utilization during exercise after high-altitude acclimation: A new perspective. *Proc Natl Acad Sci U S A* 95: 10288–10293, 1998. doi: 10.1073/pnas.95.17.10288.

36. **McClelland GB**, **Hochachka PW**, **Weber JM**. Effect of high-altitude acclimation on NEFA turnover and lipid utilization during exercise in rats. *Am J Physiol* 277: E1095-102, 1999.

37. **McClelland GB**, **Lyons SA**, **Robertson CE**. Fuel use in mammals: Conserved patterns and evolved strategies for aerobic locomotion and thermogenesis. *Integr Comp Biol* 57: 231–239, 2017. doi: 10.1093/icb/icx075.

38. **McClelland GB**, **Scott GR**. Evolved Mechanisms of Aerobic Performance and Hypoxia Resistance in High-Altitude Natives. *Annu Rev Physiol* 81: 561–583, 2019. doi: 10.1146/annurev-physiol-021317-121527.

39. **McCue MD**, **Albach A**, **Salazar G**. Previous repeated exposure to food limitation enables rats to spare lipid stores during prolonged starvation. *Physiol Biochem Zool* 90: 63–74, 2017. doi: 10.1086/689323.

683 40. **McCue MD**, **McWilliams SR**, **Pinshow B**. Ontogeny and nutritional status influence
684 oxidative kinetics of nutrients and whole-animal bioenergetics in zebra finches,
685 Taeniopygia guttata: New applications for 13C breath testing. *Physiol Biochem Zool* 84:
686 32–42, 2011. doi: 10.1086/657285.
687 41. **McCue MD**, **Pollock ED**. Measurements of substrate oxidation using 13CO2-breath
688 testing reveals shifts in fuel mix during starvation. *J Comp Physiol B Biochem Syst*
689 *Environ Physiol* 183: 1039–1052, 2013. doi: 10.1007/s00360-013-0774-z.
690 42. **Mccue MD**, **Voigt CC**, **Jefimow M**, **Wojciechowski MS**. Thermal acclimation and
691 nutritional history affect the oxidation of different classes of exogenous nutrients in
692 Siberian hamsters, Phodopus sungorus. *J Exp Zool Part A Ecol Genet Physiol* 321: 503–
693 514, 2014. doi: 10.1002/jez.1882.
694 43. **McCue MD**, **Welch KC**. 13C-Breath testing in animals: theory, applications, and future
695 directions. *J Comp Physiol B* 186(3): 265-285, 2016.
696 44. **Moriya K**, **Leblanc J**, **Arnold J**. Effects of Exercise and Intermittent Cold Exposure on
697 Shivering and Nonshivering Thermogenesis in Rats. *Jpn J Physiol* 37: 715–727, 1987.
698 45. **Nespolo RF**, **Opazo JC**, **Rosenmann M**, **Bozinovic F**. Thermal acclimation, maximum
699 metabolic rate, and nonshivering thermogenesis of Phyllotis xanthopygus (Rodentia) in
700 the Andes mountains. *J Mammal* 80: 742–748, 1999. doi: 10.2307/1383243.
701 46. **Newstead CG**. The relationship between ventilation and oxygen consumption in man is
702 the same during both moderate exercise and shivering. *J Physiol* 383: 455–459, 1987. doi:
703 10.1113/jphysiol.1987.sp016420.
704 47. **Price ER**, **Armstrong C**, **Guglielmo CG**, **Staples JF**. Selective Mobilization of
705 Saturated Fatty Acids in Isolated Adipocytes of Hibernating 13-Lined Ground Squirrels

Ictidomys tridecemlineatus. *Physiol Biochem Zool* 86: 205–212, 2013. doi: 10.1086/668892.

48. **Rezende EL**. Cold-acclimation in Peromyscus: temporal effects and individual variation in maximum metabolism and ventilatory traits. *J Exp Biol* 207(2): 295-305, 2004.

49. **Roberts TJ**, **Weber JM**, **Hoppeler H**, **Weibel ER**, **Taylor CR**. Design of the oxygen and substrate pathways. II. Defining the upper limits of carbohydrate and fat oxidation. *J Exp Biol* 199: 1651–1658, 1996.

50. **Robertson CE**, **McClelland GB**. Developmental delay in shivering limits thermogenic capacity in juvenile high-altitude deer mice (Peromyscus maniculatus). *J Exp Biol* 222, 2019. doi: 10.1242/jeb.210963.

51. **Rosenmann MS**, **Morrison PR**. Maximum oxygen consumption and heat loss facilitation in small homeotherms by He-O2. *Amer J Phsyiol* 226: 490–495, 1974.

52. **Schippers MP**, **LeMoine CMR**, **McClelland GB**. Patterns of fuel use during locomotion in mammals revisited: The importance of aerobic scope. *J Exp Biol* 217: 3193–3196, 2014. doi: 10.1242/jeb.099432.

53. **Schippers MP**, **Ramirez O**, **Arana M**, **Pinedo-Bernal P**, **McClelland GB**. Increase in carbohydrate utilization in high-altitude andean mice. *Curr Biol* 22: 2350–2354, 2012. doi: 10.1016/j.cub.2012.10.043.

54. **Scholander PF, Hock R, Walters V, Irving L.** Adaptation to cold in arctic and tropical mammals and birds in relation to body temperature, insulation, and basal metabolic rate. *Biol Bull* 99(2): 259-271, 1950.

55. **Sokolović M**, **Wehkamp D**, **Sokolović A**, **Vermeulen J**, **Gilhuijs-Pederson LA**, **van Haaften RIM**, **Nikolsky Y**, **Evelo CTA**, **van Kampen AHC**, **Hakvoort TBM**, **Lamers**

WH. Fasting induces a biphasic adaptive metabolic response in murine small intestine. *BMC Genomics* 8: 1–18, 2007. doi: 10.1186/1471-2164-8-361.

56. **Stephens FB**. Does skeletal muscle carnitine availability influence fuel selection during exercise? *Proc Nutr Soc* 77: 11–19, 2018. doi: 10.1017/S0029665117003937.

57. **Tate KB**, **Ivy CM**, **Velotta JP**, **Storz JF**, **McClelland GB**, **Cheviron ZA**, **Scott GR**. Circulatory mechanisms underlying adaptive increases in thermogenic capacity in high-altitude deer mice. *J Exp Biol* 220(20): 3616-3620, 2017.

58. **Tate KB**, **Wearing OH**, **Ivy CM**, **Cheviron ZA**, **Storz JF**, **McClelland GB**, **Scott GR**. Coordinated changes across the O2 transport pathway underlie adaptive increases in thermogenic capacity in high-altitude deer mice. *P Biol Sci* 287: 20192750, 2020. doi: 10.1098/rspb.2019.2750.

59. **Team RC**. R: a language and environment for statistical computing [Online]. Wienna, Austria: R Foundation for Statistical Computing. http://www.r-project.org [2013].

60. **Templeman NM**, **Schutz H**, **Garland T**, **McClelland GB**. Do mice bred selectively for high locomotor activity have a greater reliance on lipids to power submaximal aerobic exercise? *AJP Regul Integr Comp Physiol* 303: R101–R111, 2012. doi: 10.1152/ajpregu.00511.2011.

61. **Vaillancourt E**, **Haman F**, **Weber JM**. Fuel selection in Wistar rats exposed to cold: Shivering thermogenesis diverts fatty acids from re-esterification to oxidation. *J Physiol* 587: 4349–4359, 2009. doi: 10.1113/jphysiol.2009.175331.

62. **Van Sant MJ**, **Hammond KA**. Contribution of Shivering and Nonshivering Thermogenesis to Thermogenic Capacity for the Deer Mouse (*Peromyscus maniculatus*). *Physiol Biochem Zool* 81: 605–611, 2008. doi: 10.1086/588175.

752 63. **Weber JM**. Metabolic fuels: Regulating fluxes to select mix. *J Exp Biol* 214: 286–294,
753 2011. doi: 10.1242/jeb.047050.
754 64. **Weber JM**, **Brichon G**, **Zwingelstein G**, **Mcclelland G**, **Saucedo C**, **Weibel ER**, **Taylor**
755 **CR**. Design of the oxygen and substrate pathways. IV. Partitioning energy provision from
756 fatty acids. *J Exp Biol* 199: 1667–1674, 1996.
757 65. **Weber JM**, **Haman F**. Oxidative fuel selection: adjusting mix and flux to stay alive. *Int*
758 *Congr Ser* 1275: 22–31, 2004. doi: 10.1016/j.ics.2004.09.043.
759 66. **Weibel ER**, **Taylor CR**, **Weber JM**, **Vock R**, **Roberts TJ**, **Hoppeler H**. Design of the
760 oxygen and substrate pathways. VII. Different structural limits for oxygen and substrate
761 supply to muscle mitochondria. *J Exp Biol* 199: 1699–1709, 1996.
762 67. **White CR**, **Portugal SJ**, **Martin GR**, **Butler PJ**. Respirometry: Anhydrous drierite
763 equilibrates with carbon dioxide and increases washout times. *Physiol Biochem Zool* 79:
764 977–980, 2006. doi: 10.1086/505994.
765 68. **Withers PC**. Measurement of VO2, VCO2, and evaporative water loss with a flow-
766 through mask. *J Appl Phyiol* 42(1):120-123, 1977.
767 69. **Withers PC**, **Casey TM**, **Casey KK**. Allometry of respiratory and haematological
768 parameters of arctic mammal. *Comp Biochem Phyiol A* 64(3): 343-350, 1979.
769 70. **Yu CCW**, **McManus AM**, **Li AM**, **Sung RYT**, **Armstrong N**. Cardiopulmonary
770 exercise testing in children. *Hong Kong J Paediatr* 15: 35–47, 2010. doi:
771 10.1378/chest.120.1.81.

772
773
774
775
776
777

778 **Figure Captions**
779
780
781 **Figure 1. Oxygen consumption ($\dot{V}O_2$) (in ml g^{-1} min^{-1}) (A) and Respiratory Exchange Ratio**
782 **(RER= $\dot{V}CO_2/\dot{V}O_2$) (B) of first-generation laboratory born and raised highland and**
783 **lowland *Peromyscus mice*, acclimated to control warm normoxia (23°C, 21 kPa O_2; WN) or**
784 **cold hypoxia (5°C, 21 kPa O_2; CH), and then exposed acutely to ambient temperatures of**
785 **30°C and 0°C.** A) $\dot{V}O_2$ showed a significant effect of ambient temperature ($F_{1,79}$ = 376.12,
786 P<0.001), and population ($F_{2,79}$ = 11.48, P<0.001), while controlling for differences in body mass
787 ($F_{1,79}$ = 16.08, P<0.001). At 0°C there was a significant population effect ($F_{2,39}$ = 5.69, P=0.007).
788 At 30°C there was a main effect of population on $\dot{V}O_2$ ($F_{2,39}$ = 7.59, P=0.002). B) For RER there
789 was a significant population x acclimation interaction ($F_{2,80}$ = 6.12, P=0.003). At 30°C there was
790 a significant population x acclimation interaction ($F_{2,40}$ = 4.33, P=0.020). Symbols representing
791 significant differences result from Holm Sidak post hoc tests (p<0.05, within a given test
792 temperature). ‡Significant difference between test temperatures. *Highland and lowland deer
793 mice are significantly different than white-footed mice. †Significant difference between CH
794 lowlanders and CH white-footed mice within 30°C. N=5 for WN and CH white-footed mice; N=
795 10 and 9 for WN and CH lowland deer mice, respectively; N= 9 and 8 for WN and CH highland
796 deer mice, respectively. Data are presented as mean ± SEM.
797
798
799

800 **Figure 2. Whole-animal lipid oxidation rates (in µmol g^{-1} h^{-1}) (A), rates of [^{13}C]-palmitate**
801 **oxidation (in nmol g^{-1} h^{-1}) (B) and concentrations of circulating plasma Non-Esterified**
802 **Fatty Acids (NEFAs, in µmol L^{-1}) (C) of first-generation laboratory born and raised**
803 **highland and lowland *Peromyscus mice*, acclimated to control warm normoxia (23°C, 21**
804 **kPa O_2; WN) or cold hypoxia (5°C, 21 kPa O_2; CH), and exposed acutely to ambient**
805 **temperatures of 30°C and 0°C.** A) Whole-animal lipid oxidation rate showed a significant
806 effect of ambient temperature ($F_{1,79}$ = 123.77, P<0.001) and population ($F_{2,79}$ = 3.51, P=0.035)
807 while controlling for differences in body mass ($F_{1,79}$ = 3.95, P=0.050). At 30°C there was a
808 significant population effect ($F_{2,39}$ = 5.88, P=0.006) while controlling for body mass ($F_{1,39}$ =
809 0.236, P=0.630). N=5 for WN and CH white-footed mice; N= 10 and 9 for WN and CH lowland
810 deer mice, respectively; N= 9 and 8 for WN and CH highland deer mice, respectively. B) [^{13}C]-
811 palmitate oxidation showed a significant effect of ambient temperature ($F_{1,35}$ = 157.30, P<0.001)
812 and acclimation ($F_{1,35}$ = 12.21, P=0.001) while controlling for body mass ($F_{1,35}$ = 0.044,
813 P=0.835). At 30°C there was a significant population x acclimation interaction ($F_{1,17}$ = 6.59,
814 P=0.020), and significant acclimation effect ($F_{1,17}$ = 14.82, P=0.001), all while controlling for
815 body mass ($F_{1,17}$ = 0.000, P=0.999). Symbols representing significant differences result from
816 Holm Sidak post hoc tests (p<0.05, within a given test temperature). ‡Significant difference
817 between test temperatures. *Highland and lowland deer mice are significantly different than
818 white-footed mice. †Significant difference between highland acclimation groups within 30°C. A)
819 N=5 for WN and CH white-footed mice; N= 10 and 9 for WN and CH lowland deer mice,
820 respectively; N= 9 and 8 for WN and CH highland deer mice, respectively. B) N=7 and 5 for
821 WN and CH lowland deer mice, respectively; N= 8 and 4 for WN and CH highland deer mice,
822 respectively. C) N=8-9 for WN and 5 for CH lowland deer mice, respectively; N= 9-10 and 4 for
823 WN and CH highland deer mice, respectively. All data are presented as mean ± SEM.

824 **Figure 3. Concentrations of individual plasma fatty acids (in μmol L^{-1}) of first-generation**
825 **laboratory born and raised highland and lowland deer mice (*Peromyscus maniculatus*),**
826 **acclimated to control warm normoxia (23°C, 21 kPa O_2; WN) or cold hypoxia (5°C, 21 kPa**
827 **O_2; CH), acutely exposed to ambient temperatures of 30°C and 0°C.** Palmitoleic acid (16:1)
828 (B); at 0°C there was a significant acclimation effect ($F_{1,23}$ = 12.99, P=0.001) while at 30°C there
829 was a significant population effect ($F_{1,23}$ = 6.70, P=0.015). Elaidic acid (18:1n9t) (D); at 30°C
830 there was a significant population effect ($F_{1,23}$ = 4.96, P=0.036). Oleic acid (18:1n9c) (E); at 0°C
831 there was a significant acclimation effect ($F_{1,23}$ = 19.66, P<0.001) while at 30°C there was a
832 significant population effect ($F_{1,23}$ = 5.77, P=0.025) and acclimation effect ($F_{1,23}$ = 4.91,
833 P=0.037). Symbols representing significant differences result from Holm Sidak post hoc tests
834 (p<0.05, within a given test temperature). *Main population effect within a given test
835 temperature. †Main acclimation effect within a given test temperature. N=8-9 for WN and 5 for
836 CH lowland deer mice, respectively; N= 9-10 and 4 for WN and CH highland deer mice,
837 respectively. Data are presented as mean ± SEM.
838

839

840 **Figure 4. Cold-induced maximal oxygen consumption ($\dot{V}O_2$) (in ml g^{-1} min^{-1}) (A) with the**
841 **corresponding Respiratory Exchange Ratios (RER= $\dot{V}CO_2/\dot{V}O_2$) (B) whole-animal lipid**
842 **oxidation rates (in μmol g^{-1} hr^{-1}) (C) of first-generation laboratory born and raised**
843 **highland and lowland *Peromyscus* mice, acclimated to control warm normoxia (23°C, 21**
844 **kPa O_2;WN) or cold hypoxia (5°C, 21 kPa O_2; CH), acutely exposed to normoxia (21% O_2)**
845 **or hypoxia (12% O_2).** A) There was a significant effect of condition on cold-induced $\dot{V}O_2$max
846 ($F_{1,135}$ = 353.22, P<0.001) while controlling for the effects of body mass ($F_{1,135}$ = 16.93,
847 P<0.001). White-footed mice weighed significantly more than both highland and lowland deer
848 mice, regardless of acclimation environment (p<0.05). There was a significant effect of
849 acclimation on cold-induced $\dot{V}O_2$max in normoxic ($F_{1,39}$ = 48.85, P<0.001) and hypoxic ($F_{1,95}$ =
850 170.33, P<0.001) conditions. B) Under normoxic conditions, there was a significant population ×
851 acclimation interaction in RER ($F_{2,40}$ = 4.10, P=0.024). C) Lipid oxidation rates showed a
852 significant effect of $\dot{V}O_2$max condition ($F_{1,135}$ = 43.74, P<0.001) and acclimation ($F_{1,135}$ = 55.00,
853 P<0.001). There was a significant interaction between population, acclimation and $\dot{V}O_2$max
854 condition ($F_{1,135}$ =6.93, P=0.001). All factors had mass as a covariate ($F_{1,135}$ = 6.33, P=0.013). In
855 normoxia, there was a significant interaction between population and acclimation ($F_{2,39}$ = 4.62,
856 P=0.016) while controlling for mass ($F_{1,39}$ = 0.202, P=0.656). In hypoxia, there was a significant
857 effect of population ($F_{2,95}$ = 3.16, P=0.047) and acclimation ($F_{1,95}$ = 44.06, P<0.001) whilst
858 controlling for differences in body mass ($F_{1,95}$ = 16.68, P<0.001). Symbols representing
859 significant differences result from Holm Sidak post hoc tests (p<0.05, within a given $\dot{V}O_2$max
860 condition). ‡Significant difference between cold-induced $\dot{V}O_2$max conditions. *Highlanders
861 significantly differ from lowland deer mice within hypoxic cold-induced $\dot{V}O_2$max conditions.
862 †Main acclimation effect within a given cold-induced $\dot{V}O_2$max condition. ¥ WN highland deer
863 mice significantly differ from CH highland and WN lowland deer mice, within the normoxic
864 $\dot{V}O_2$max condition. ^{X}WN highlanders and WN white-footed mice significantly differ from CH
865 highlanders within the normoxic $\dot{V}O_2$max condition. N=5-15 for WN white-footed mice (mass
866 (in g) = 24.8 ± 1.7 and 26.5 ± 1.0 for normoxia and hypoxia, respectively) and CH white-footed
867 mice (mass (in g) = 27.6 ± 1.7 and 26.7 ± 1.0 for normoxia and hypoxia, respectively). N= 9-19

868 for WN lowland deer mice (mass (in g) = 20.8 ±1.2 and 20.7 ±1.0 for normoxia and hypoxia,
869 respectively) and CH lowland deer mice (mass (in g) = 17.9 ± 1.3 and 20.2 ± 0.9 for normoxia
870 and hypoxia, respectively). N= 8-21 for WN highland deer mice (mass (in g) = 22.0 ± 1.3 and
871 20.3 ± 0.8 for normoxia and hypoxia, respectively) and CH highland deer mice (mass (in g) =
872 19.5 ± 1.3 and 21.5 ± 0.9 for normoxia and hypoxia, respectively). Data are presented as mean ±
873 SEM. Mass and $\dot{V}O_2$max in hypoxia data from Tate et al., 2020.
874

875

876 **Figure 5.** Mass-specific lipid oxidation rates as a function of metabolic rate at 30^{o}C, 15^{o}C, 0^{o}C
877 and normoxic cold-induced $\dot{V}O_2$max in warm normoxia (23^{o}C, 21 kPa O_2) and cold hypoxia
878 (5^{o}C, 21 kPa O_2) acclimated high-altitude deer mice (this study) compared to those during
879 submaximal aerobic exercise in running humans (1), dogs (49) and deer mice (33) and with
880 moderate shivering thermogenesis in rats (dark circle represents lipid oxidation but only during
881 shivering thermogenesis) (61).
882

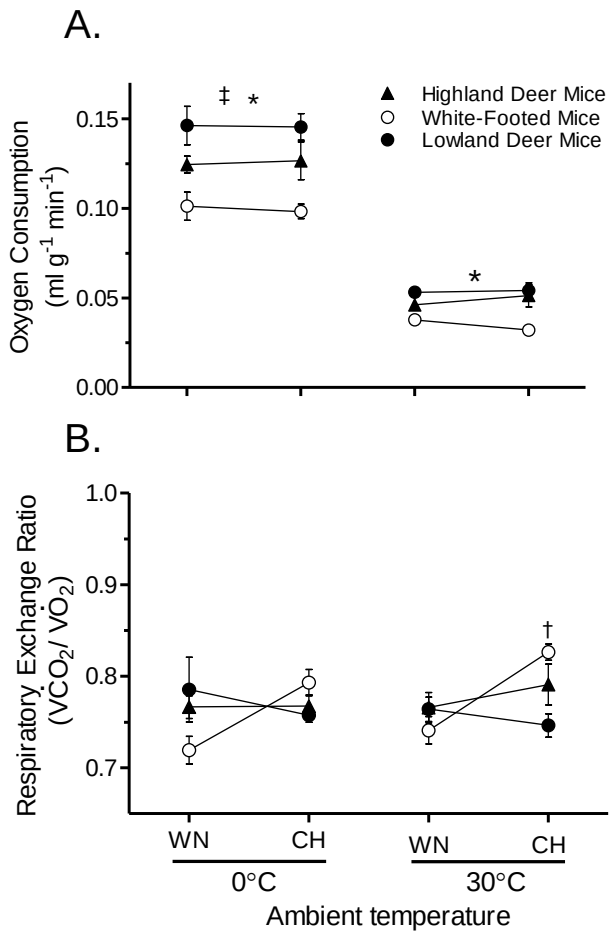

Fig.1

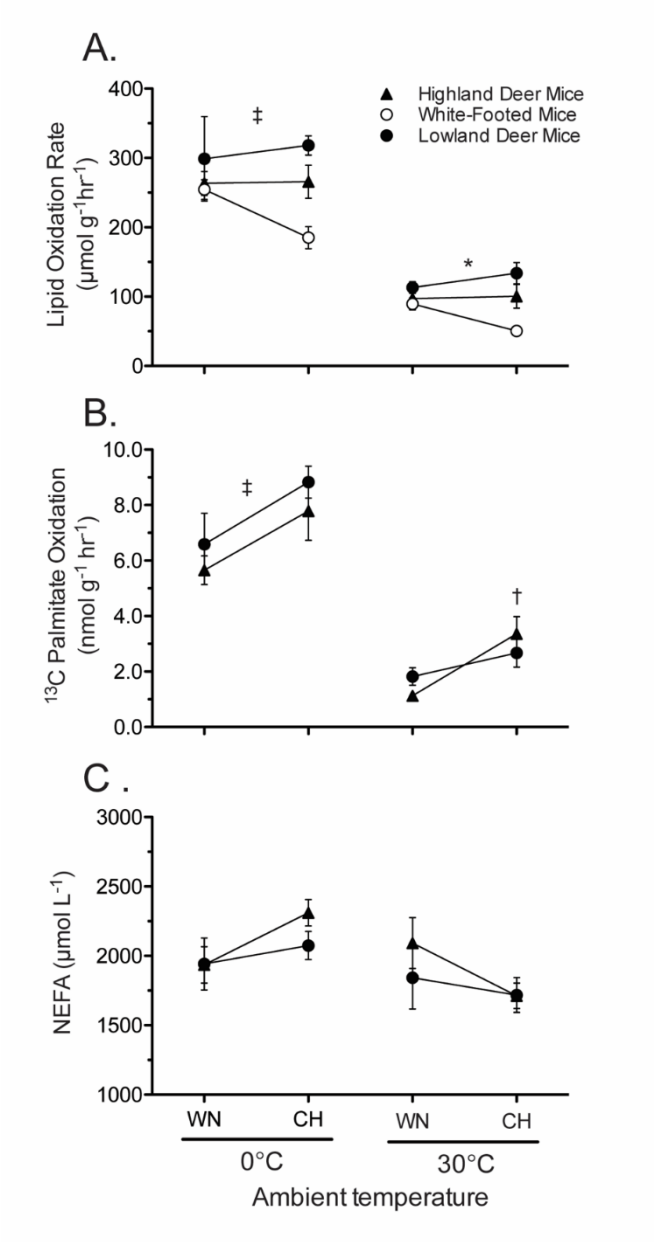

Fig.2

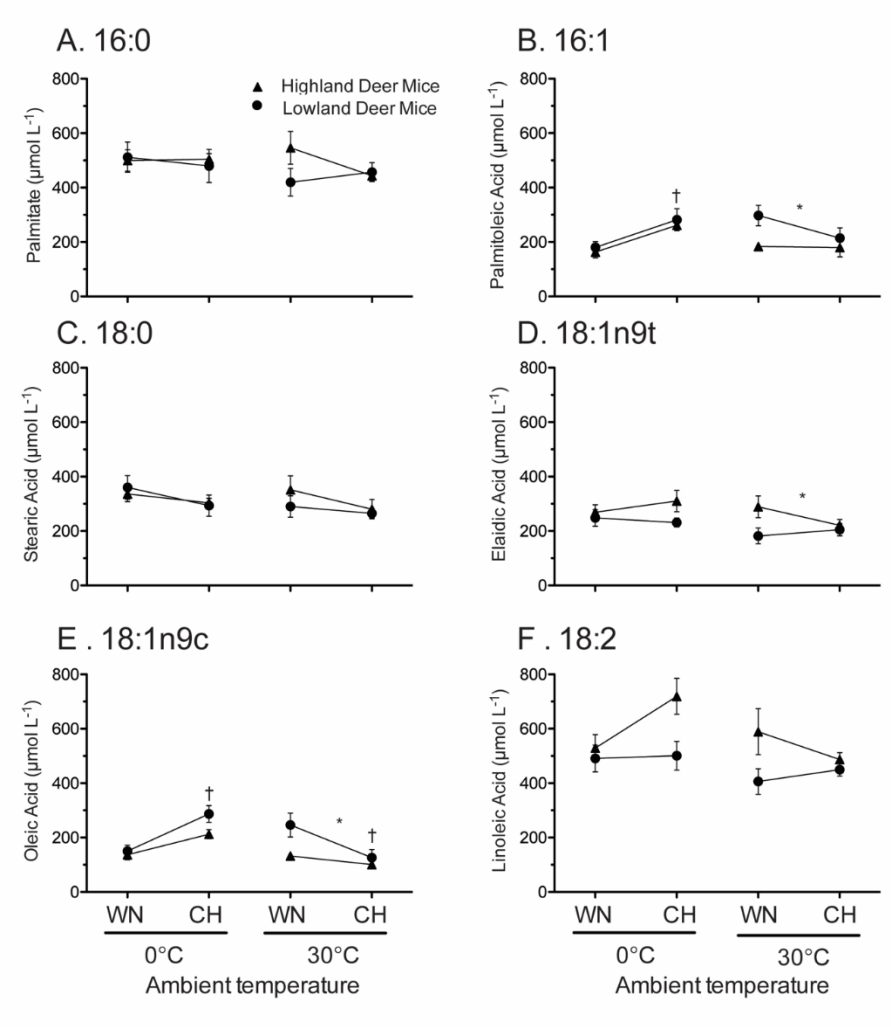

Fig 3

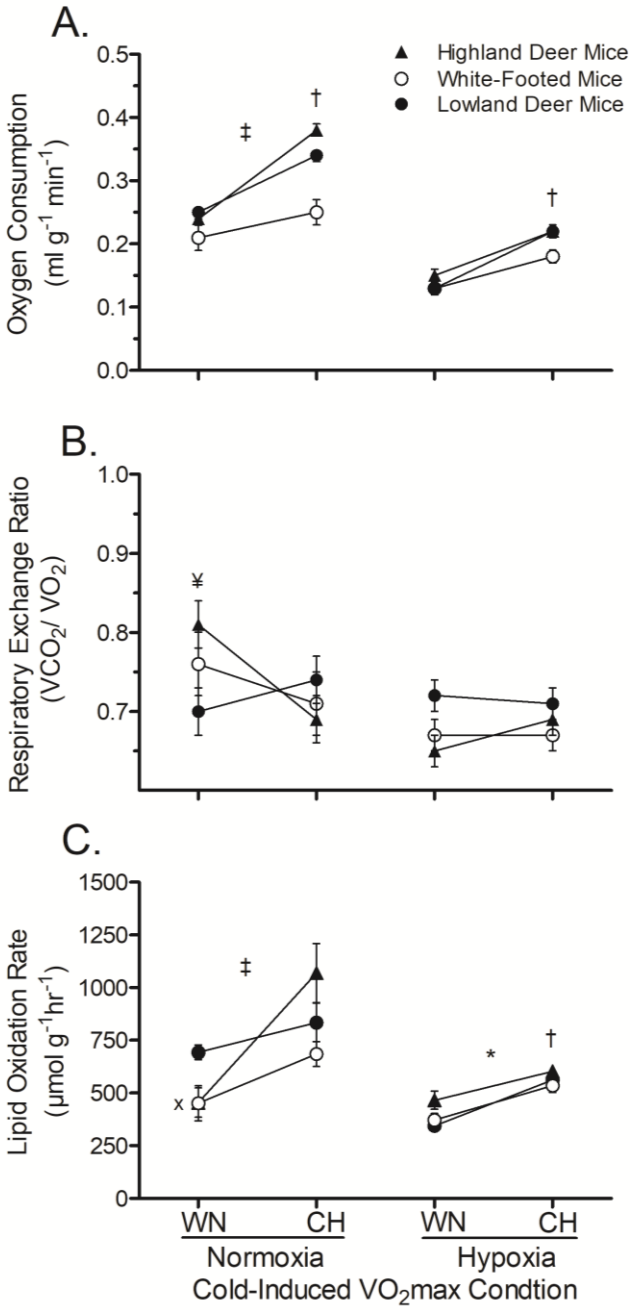

Fig 4.

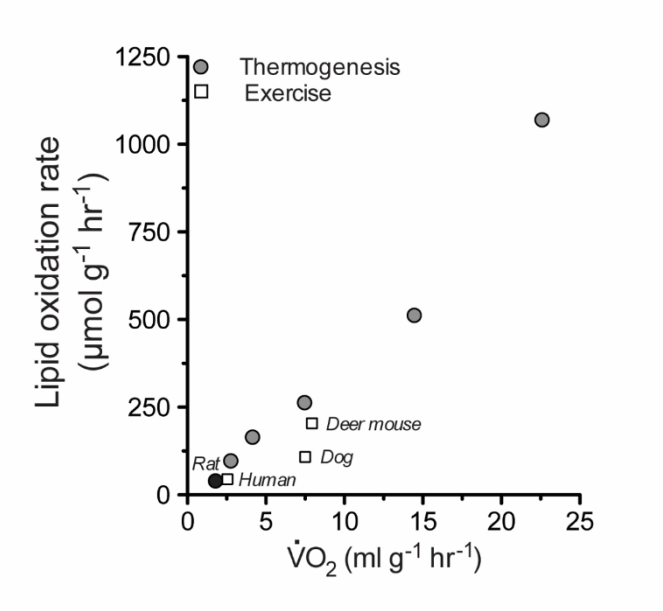

Fig 5.

Table 1. Body mass, change in body temperature (ΔT_b) and thermal conductance (C) of first-generation laboratory born and raised highland and lowland *Peromyscus* mice, acclimated to control (23°C, 21 kPa O_2; WN) or cold hypoxia (5°C, 21 kPa O2; CH), exposed to ambient temperatures of 30°C and 0°C. Values are means ± SEM.

	Lowland (*P. leucopus*)				Lowland (*P. maniculatus*)				Highland (*P. maniculatus*)			
	Warm Normoxia		Cold Hypoxia		Warm Normoxia		Cold Hypoxia		Warm Normoxia		Cold Hypoxia	
	30°C	0 °C	30 °C	0 °C	30 °C	0 °C	30 °C	0 °C	30 °C	0 °C	30 °C	0 °C
Mass (g)	21.7 ± 1.7†	23.6 ± 1.6†	26.3 ± 0.6†	26.6 ± 0.9†	20.4 ± 1.2	19.9 ± 1.2	16.9 ± 0.6	17.2 ± 0.6	20.5 ± 1.3	20.7 ± 1.2	18.4 ± 0.7	18.8 ± 0.8
ΔT_b (°C)	-0.31 ± 0.5	-2.11 ± 0.9†	0.61 ± 0.61	-1.04 ± 0.4†	0.64 ± 0.33	0.57 ± 0.33	1.24 ± 0.35	0.18 ± 0.27	0.13 ± 0.42	0.60 ± 0.35	0.93 ± 0.56	1.24 ± 0.45
C (ml O_2 g^{-1} hr^{-1} $°C^{-1}$)	0.28 ± 0.01†	0.17 ± 0.01*†	0.24 ± 0.01†	0.16 ± 0.01*†	0.39 ± 0.02	0.23 ± 0.02*	0.39 ± 0.02	0.23 ± 0.01*	0.39 ± 0.03	0.20 ± 0.01*	0.39 ± 0.03	0.20 ± 0.02*

Symbols representing significant differences result from Holm Sidak post hoc tests ($p<0.05$, within a given test temperature).

†Significantly different from highland and lowland deer mice within a given temperature.

*Significantly different from 30°C